

A POSSIBLE PHENOMENOLOGICAL BARRIER PENETRATION
DESCRIPTION FOR FAR SUB-BARRIER $^{58}\text{Ni}+^{58}\text{Ni}$ FUSION SYSTEM

MOSTAFA M. SHALABY, MOHAMED N. KHALIL and HALA M. KHALIL*

Physics Department, Faculty of Science, Ain Shams University

**Physics Department, University College for Girls, Ain Shams University, Cairo, Egypt*

Received 10 June 1982

Revised manuscript received 25 October 1982

UDC 539.17

Original scientific paper

The one-dimensional barrier penetration model was successfully applied in description of excitation function for complete fusion of $^{58}\text{Ni}+^{58}\text{Ni}$ system, particularly at far sub-barrier energies. Using different nuclear potentials (KNS, proximity, empirical SWW and NGÖ) a strong sensitivity to changes in nuclear radius parameter r_0 ($\Delta r_0 < 0.065$) was established for fitting this high precision data. The minor monotonic increase of r_0 with decreasing energy was manifested in geometry of the barrier and the attractive nature of the nuclear potentials (involved) in the surface region.

1. Introduction

The increasing body of high precision data measurements of excitation function for complete fusion of massive nuclei at near and sub-barrier energies are now available (Beckerman et al.^{1,2}), to provide insight into the interplay between fusion dynamics and the underlying nuclear structure. A prototype example is the $^{58}\text{Ni}+^{58}\text{Ni}$ complete fusion data at $187.6 < E_{lab} < 220$ MeV. The cross-sections for complete fusion at sub-barrier energies are found to be far greater (more than two orders of magnitude) than those predicted by the standard one-dimensional barrier penetration model (Beckerman et al.²). On the other hand, fusion of light system as $^{14}\text{N}+^{16}\text{O}$ (Switkowski et al.³) and $^{32}\text{S}+^{27}\text{Al}$ (Gutbrod et al.⁴) are

described in a very satisfactory way using this model (Krappe⁵). The large sub-barrier fusion cross-sections of massive nuclei was tried to be explained within a liquid drop framework as a consequence of zero point motion. Landowne and Nix⁶ presented calculations for $^{58}\text{Ni} + ^{58}\text{Ni}$ system which took into account average dynamic deformations as well as zero point motion. Their results were an excitation function similar to that for penetration of a one-dimensional barrier by spherical nuclei. The substantially increase in fusion cross section arising from zero-point motion is, however, insufficient to explain the observed large sub-barrier fusion data. A phenomenological analysis based on one-dimensional barrier penetration model, employed the WKB method (in calculating the transmission coefficient) and introduce a radially dependent effective mass has been carried out by Beckerman et al.⁷. Although a close agreement to $^{58}\text{Ni} + ^{58}\text{Ni}$ fusion data was obtained, still at far sub-barrier energy better fit to data is needed. The extent to which the simple one-dimensional barrier (approximated to inverted harmonic oscillator) model can account for sub-barrier fusion data and strong sensitivity of the $^{58}\text{Ni} + ^{58}\text{Ni}$ high precision fusion data to type and geometry of nuclear potential involved has been studied by introducing a minor monotonic decrease of nuclear radius parameter r_0 , with energy.

2. Method of analysis

A phenomenological analysis based on adiabatic, one-dimensional barrier penetration model is presented. The condition for fusion is that, there exists a maximum in the effective real potential $V(r, l)$ and the cross-section for complete fusion is obtained from partial wave summation

$$\sigma^{cf} = \pi\lambda^2 \sum_l (2l + 1) T_l. \quad (1)$$

The contribution of each partial wave (l) to σ^{cf} was determined only by the transmission coefficient $T_l(E_{cm})$ which means that probability (P_l) of fusion of partial wave l , that penetrates the effective real barrier with penetrability T_l , is set equal to unity. $T_l(E_{cm})$ for each partial wave l was calculated with the Hill-Wheeler⁸ relation

$$T_l(E_{cm}) = \left[1 + \exp\left(\frac{2\pi}{\hbar\omega} (V_l(R_l) - E_{cm})\right) \right]^{-1} \quad (2)$$

where the shape of the interaction barrier was approximated to that of an inverted harmonic oscillator, $V_l(R_l)$ is its height for the l -th partial wave, R_l is its radial position and $\hbar\omega$ is its curvature given by

$$\hbar\omega = \left| \frac{\hbar^2}{\mu} \frac{d^2 V(r, l)}{dr^2} \right|_{r=R_l}^{1/2} \quad (3)$$

R_l corresponding to the maximum in the potential $V(r, l)$ and μ is the reduced mass of the system. The interaction potential $V(r, l)$ is the usual sum of the coulomb, nuclear and centrifugal potentials

$$V(r, l) = V_{coul}(r) + V_{nucl}(r) + \frac{\hbar^2 l(l+1)}{2\mu r^2}. \quad (4)$$

a) *Coulomb potential*

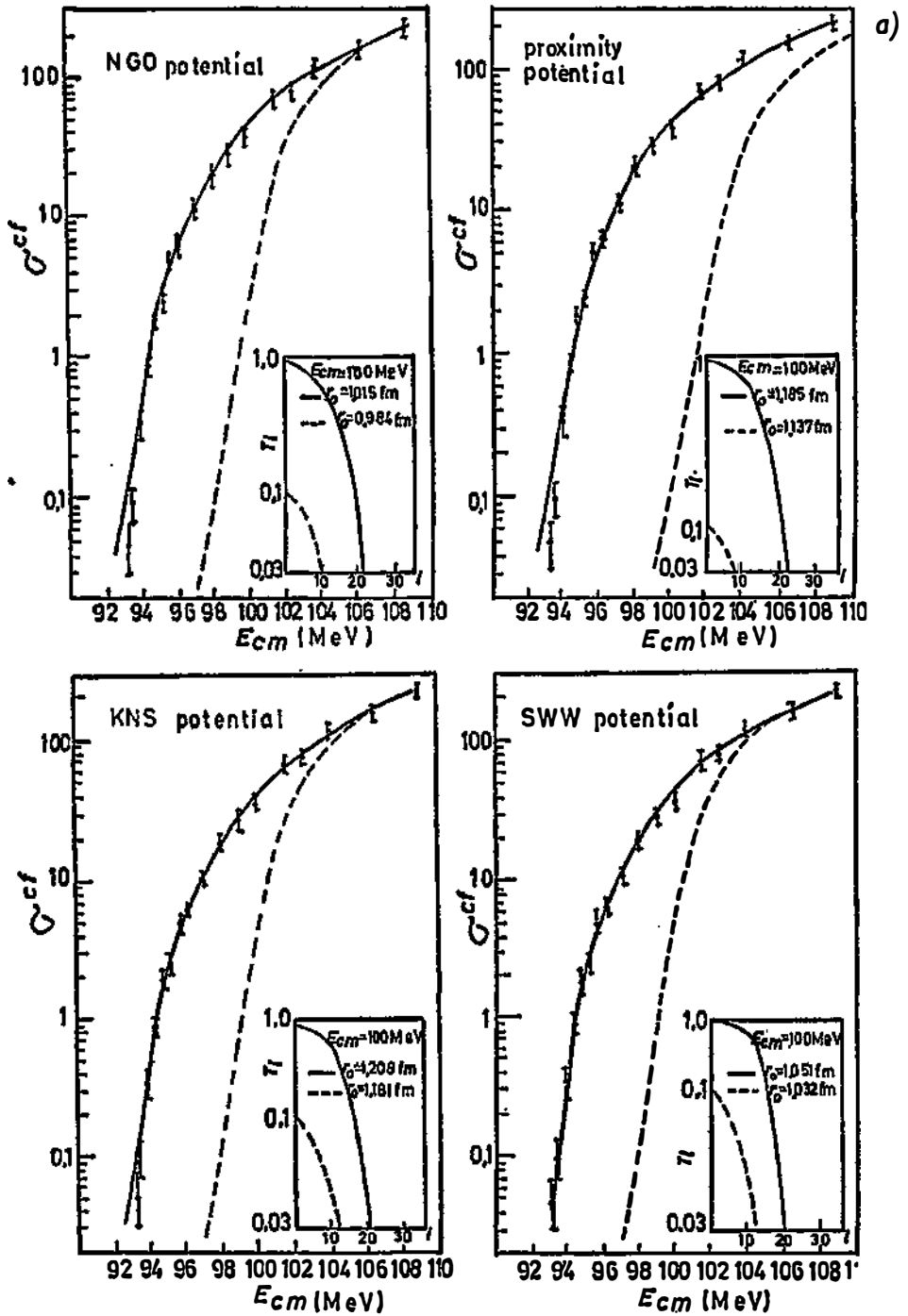
The form of the coulomb potential used was that of a point plus spherical charge distribution. Preliminary results shows that use of the phenomenological coulomb potential of Bondorf et al.⁹⁾ makes no significant differences within the involved energy range.

b) *Nuclear potential*

Three widely used surface-surface potentials are applied in the present analysis: (i) The unified KNS potential (Krappe et al.¹⁰⁾) as a most recent generalization of liquid drop model, (ii) The proximity potential (Blocki et al.¹¹⁾) where ion-ion potential was calculated in terms of interaction energy per unit area between two semiinfinite nuclei, (iii) The empirical Saxon-Woods potential SWW¹²⁾, where parameters involved are obtained from boundary conditions following the liquid drop model. Two of these potentials are strongly attractive in the deep nuclear interior (SWW) and (KNS) while the proximity potential is of hard core repulsive nature. A fourth potential, has the same latter feature, and deduced by Ngô et al.¹³⁾ from the energy density formalism, was also tried in the present analysis.

3. Results and discussion

In Fig. 1a calculation of σ^{cf} using equation (1) fitted to the experimental data of the excitation function for complete fusion of $^{58}\text{Ni} + ^{58}\text{Ni}$ is shown. It is clear that quality of fit was strongly improved by introducing minor energy dependence of the nuclear radius parameter r_0 , compared with both calculations of Beckerman et al.²⁾ using constant r_0 and that of Landowne and Nix⁶⁾ (Fig. 1b) using one-dimensional barrier corresponding to spherical nuclei and two-dimensional potential-energy surface. The systematic smooth (very slight) increase of r_0 with decreasing energy is shown in Fig. 2. Associated with each of the four nuclear potentials applied in the present analysis a display for the corresponding $T_l(E_{cm})$ at a mid $E_{cm} = 100$ MeV is also shown in Fig. 1a at two adjacent r_0 values. Another probing of fusion data to details of the nuclear potential involved is shown in Fig. 3. Increasing r_0 (with decreasing energy) produced a slight more attractive nuclear potential in the tail region, with negligible changes in the far interior region for the SWW and KNS potential (non hard core potentials). This is the possible energy dependence in geometry (parameters) of the nuclear potential which are related to r_0 . Other parameters involved in these potentials such as the range of Yukawa folding function which appears in the KNS potential ($a = 0.68$ fm) were kept constant. However, this adjustment of r_0 was reflected in changes of the total interaction potential mainly in the tail region for the four different nuclear



potentials. Thus only geometry of the barrier, independent of details of nuclear potential (particularly in deep nuclear interior) whether it is of hard repulsive core or strongly attractive one, will be the principle contribution in description of fusion mechanism. This is consistent with the present analysis of fusion data in terms of the one dimensional barrier penetration model.

The quantities V_0 and $\hbar\omega_0$ that appears in Fig. 3 denote height and curvature of the S -wave interaction barrier maximum, as the most significant changes in T_1 is clearer at low partial waves. Only changes in V_0 (more generally $V_l(R_l)$)

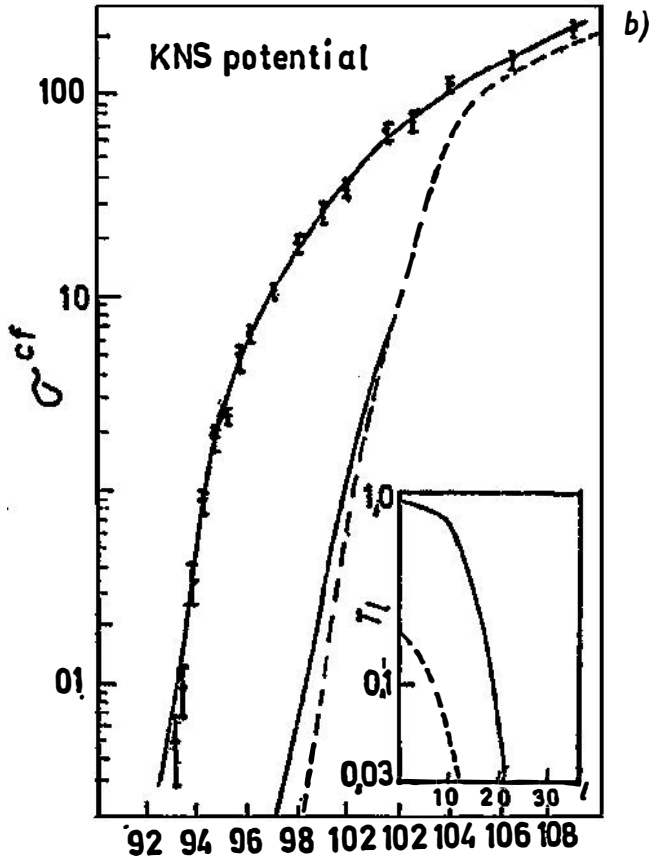


Fig. 1.a. Excitation function for complete fusion of $^{58}\text{Ni} + ^{58}\text{Ni}$. (\square) Experimental data of Beckerman et al. (1981). (—) Solid and dotted (---) curves are the adiabatic barrier penetration (model) calculations using smoothly varying (present work) and constant (Beckerman et al. 1981) radius parameter r_0 , respectively. Nuclear potentials used are NGÖ, proximity, KNS and SWW potential. A display for $T_l(E_{cm})$ at mid $E_{cm} = 100$ MeV is shown in the insert of Fig 1. associated with each of the four potentials used. The cross-section is expressed in 10^{-31} m^2 .

Fig. 1.b. Dashed curve gives the result for one-dimensional barrier corresponding to spherical nuclei and solid curve gives result for two-dimensional potential energy surface (Landowne and Nix³¹). The cross-section is expressed in 10^{-31} m^2 .

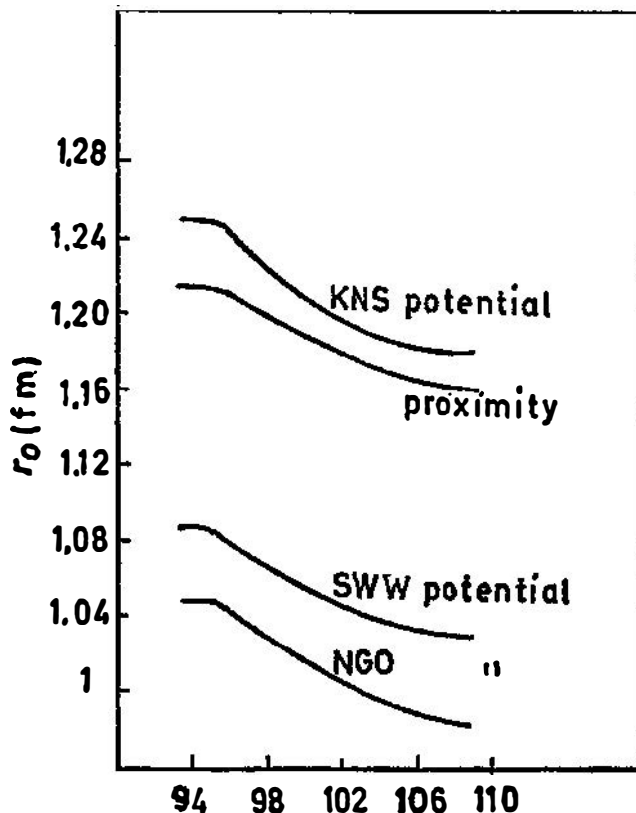


Fig. 2. Systematic smooth (very slight) increase of r_0 with decreasing energy associated with each of the four potentials used.

is the principle factor affecting T_l and causes its drastic increase from say $\cong 0.1$ up to $\cong 1.0$ (for $l = 0$).

In conclusion we find that fusion cross-sections at near barrier energies are extremely sensitive to slight changes in r_0 and a $\Delta r_0 < 0.065$ was an upper limit changes required for any of the nuclear potentials involved to fit fusion data in the energy range $187.6 < E_{lab} < 220$ MeV. As ^{58}Ni is spherical vibrational nucleus with an upper limit quadrupole deformation parameter, $\beta = 0.183^{11}$, it is possible to consider variations in r_0 (Δr_0) as a manifestation to dynamical deformations associated with fusion of $^{58}\text{Ni} + ^{58}\text{Ni}$ system. The slightly smooth increase of r_0 with decreasing energy was manifested in (i) a more attractive nuclear potential (with negligible changes away from the barrier), (ii) a depression in the maximum of the potential barrier ($V_l(R_l)$). This fusion dynamic may be an essential feature for description of the particularly far sub-barrier energy data where the slight drop of $V_l(R_l)$ relative to E_{cm} strongly effects (rising) the corresponding T_l and consequently its contribution to σ^{cf} .

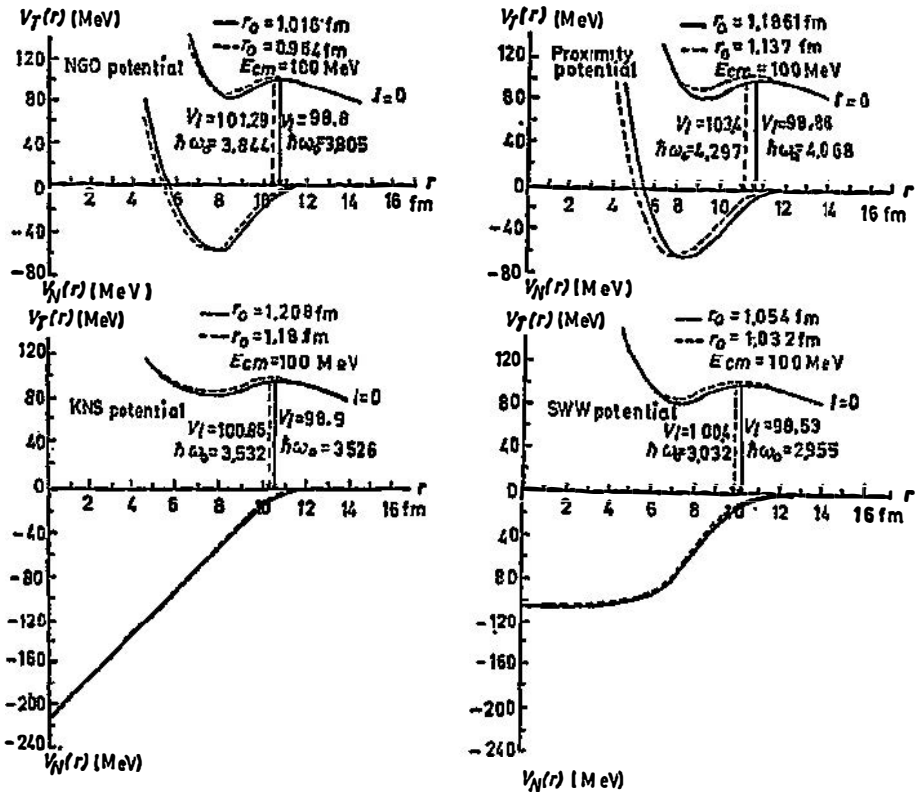


Fig. 3. The total (coulomb + nuclear + centrifugal) potential for the interaction of $^{58}\text{Ni} + ^{58}\text{Ni}$ at $l = 0$. Display for the nuclear potential used is also shown at two adjacent r_0 values together with the corresponding height (V_l) and curvature $\hbar\omega_0$ of the S -wave interaction barrier maximum.

References

- 1) M. Beckerman, M. Saloma, A. Sperduto, H. Enge, J. Ball, A. Di Rienzo, S. Gazes, Y. Chen, J. D. Molitoris and M. Nai-Feng, Phys. Rev. Lett. **45** (1950) 1472;
- 2) M. Beckerman, J. Ball, H. Enge, M. Saloma, A. Sperduto, S. Gazes, A. Di Rienzo and J. Molitoris, Phys. Rev. **C 23** (1981) 1581;
- 3) Z. Switkowski, R. Stockstad and R. Wieland, Nucl. Phys. **A 279** (1977) 502;
- 4) H. Gutbrod, N. Winn and M. Blann, Nucl. Phys. **A 213** (1973) 267;
- 5) H. Krappe, *Deep-Inelastic and fusion reactions with heavy ions*, Proceedings, Berlin (1979) p. 312;
- 6) S. Landowne and J. Nix, Nucl. Phys. **A 368** (1981) 352;
- 7) M. Beckerman, M. Saloma, A. Sperduto and J. Molitoris, (1982) preprint;
- 8) D. Hill and J. Wheeler, Phys. Rev. **C 17** (1953) 1700;
- 9) J. Bondorf, M. Sobel and D. Sperber, Phys. Rep. **C 15** (1974) 83;
- 10) H. Krappe, J. Nix and A. Sierk, Phys. Rev. Lett. **42** (1979) 215;
- 11) J. Blocki, J. Bandrup, D. Swiatecki and C. Tsang, Ann. Phys. **105** (1977) 427 and J. Randrup, Nucl. Phys. **A 307** (1978) 319;
- 12) K. Siewek-Wilczynska and J. Wilczynski, Phys. Lett. **47 B** (1978) 313;
- 13) C. Ngô, B. Tamain, M. Beiner, R. Lombard, D. Mass and D. Dembler, Nucl. Phys. **A 252** (1975) 237.

OPIS FUSIONOG SISTEMA $^{58}\text{Ni} + ^{58}\text{Ni}$ POMOĆU JEDNOSTAVNOG
MODELA POTENCIJALNOG BEDEMA

MOSTAFA M. SHALABY, MOHAMED H. KHALIL i HALA M. KHALIL*

Physics Department, Faculty of Science, Ain Shams University

**Physics Department, University College for Girls, Ain Shams University, Cairo, Egypt*

UDK 539.17

Originalni znanstveni rad

Polazi se od računanja koeficijenta transmisije kroz jednodimenzionalni potencijalni bedem. U potencijal koji sadrži coulombski, centrifugalni i nuklearni član, za nuklearni potencijal stavljaju se četiri uobičajene parametrizacije (Krappe, Blocki, Saxon-Wood, Ngô). Kako koeficijenti transmisije, a time i udarni presjeci, jako ovise o nuklearnom radijusu r_0 , to se uz pretpostavku male ovisnosti r_0 o energiji može postići dobro slaganje izračunatih udarnih presjeka sa izmjerenim vrijednostima.